GALILEO AT JUPITER: DELIVERY ACCURACY

R.J. Haw, P.G. Antreasian, E.J. Graat, T. P. McElrath, k'."]'. Nicholson

Jet Propulsion Laboratory
California Institute of I'ethnology
Pasadena CA 91109

Abstract

Analysis of doppler tracking from the Galileo spacecraft has yielded a preliminary estimate for the second order gravity field of Io, and improved upon values for the 10, and Europa masses and ephemerides, and the rotational pole, mass, and ephemeris of Jupiter. The present results are consistent with previously published results for Voyagers I and II. Mass results are expressed as [he product GM, the universal gravitational constant G times the mass in grams M of the body, in units 01' ($km^3 s^{-2}$). With these updated values, reconstructions of the encounters of the Galileo spacecraft pair (orbiter and probe) with Jupiter and Io were possible.

Introduction

In this paper we shall describe Galileo's navigation accuracies achieved during the five months preceding the Jupiter encounter for bo(h the probe and orbiter, and compare these with the corresponding theoretical predictions. Furthermore we compute new ephemerides for Jupiter, Io, and Europa. as well as estimating a second order gravity field for Io. New values for the mass of Jupiter and its rotation axis are also provided. Background information on the spacecraft and its mission to Jupiter have been well-documented in the literature [1][2][3].

Probe Targeting and Ephemeris Determination

Galileo's Jupiter encounter began with [he acclivities associated with the release of its atmosphere probe on July 13, 1995, The probe's target was defined to be an altitude of 450km above the 1 bar level of Jupiter's atmosphere (the reference ellipsoid). Targeting parameters included entry time, flight path angle with respect [o the atmosphere (relative flight path angle), and entry latitude. To prevent skipping out of the atmosphere or excessive accelerations upon entry, while maintaining radio link margins, the probe trajectory had to achieve a relative path angle of -8.60" $\pm$1.4° at a latitude of 6.57" $\pm$0.5° on December 7, 22:04:26 $\pm$ 480 seconds UTC, Jupiter True Equator of Date (JTED) [4]. These margins are in terms of the 99th centile certainty, or equivalently, 2.6σ

Probe Release Procedures

On March 23, 1995 a trajectory correction maneuver (TCM23) targetted the combined orbiter/probe spacecraft to -6.5° latitude and 240" longitude, JTED. Afterwards the spacecraft's attitude was readjusted [o establish the correct angle of attack for the probe. Next the orbiter/probe was spun-up from 2.89 rpm to approximately 10.5 rpm. And finally on July 13, 1995, the probe was ejected from the orbiter by a pre-loaded spring mechanism. These events are chronicled in Table 1.

As documented in ref. [1], navigation observables for the orbiter/probe spacecraft included two-way coherent S-bred doppler (F2) (at least seven passes per week), one-way S-band doppler (F1) when available, and approximately hi-weekly ramped-doppler ranging (prior to probe release only). Doppler coverage increased to continuous tracking during special events such as maneuvers. The F2 were weighted between 1 mm s^{-1} and 2 mm s^{-1} for 60 second averages. During probe release (and ODM), orbiter maintenance activities precluded F2 collection for several days, and F1 was utilized in its place.

The probe could not be tracked after separation from the orbiter, [bus knowledge of the probe trajectory was inferred from orbiter tracking. The strategy followed for determining the probe's orbit started with reconstructing the orbiter's trajectory to Jupiter. A long arc of nearly one year in length, from January [o December 1995, was used for this purpose, This arc was also used to estimate a new Jupiter ephemeris. Based on the orbiter reconstruction, an updated Jupiter *ephemeris,* and probe telemetry the atmosphere probes's trajectory could be reconstructed.

Table 1. Jupiter Approach Event Times

Event	Date	UTC/SCET
Spin-up for probe sep	12-Jul-95	08:17
Probe separation	13-Jul-95	05:30
Probe sep spin-down	20-Jul-95	06:33
ODM spin-up	22-Jul-95	07:04
ODM	27-Jul-95	07:00
OOM spin-down	28-Jul-95	09:32
TCM26	29-Aug-95	02:00
TCM27	17-Nov-95	18:00
TCM28	27-Nov-95	18:00
TCM28A	2-Dee-95	20:00
Europa flyby	7-Dec-95	13:09
Io flyby	7-Dee-95	17:46
Jupiter closest approach	7-Dee-95	21:54
Probe entry	7-Dee-95	22:07
SoIn-up	7-Dee-95	23:55
JO I	8-Dec-95	00:27
Spin-down	8-Dee-95	18:03

Orbiter Reconstruction and Jupiter Ephemeris Determination

Data Gleaning

l-he arc for determining the Jupiter ephemeris consisted of data from January 10 through December 7, 1995 04:16:00 UTC SCET. (This time marks the last F2 point before JOI.) Note that this arc excludes encounter (or post-encounter) data. This was intentional, to prevent aliasing the ephemeris determination with Io and JOI uncertainties.

The data remained stable during the first seven months of the. arc. In the last four months. however, increasing noise and unexplained biases (3 to 4 mhz) in the F2 produced orbit solutions with inconsistencies. The absence of the Canberra 70-meter antenna in September and October (maintenance) participated in the erosion of [he solution stability. Also, due to the southerly declination of the spacecraft (-220), northern hemisphere tracking from Madrid and Goldstone produced low elevation profiles, Given the susceptibility of tracking data under such conditions to media effects, primarily from the ionosphere, an attempt was made to estimate the error in ionospheric calibrations by modelling the ionosphere as a stochastic process with a three-day correlation time, using the same process noise as the *a priori* sigmas. This approach yielded more consistent results, and although the inconsistencies did not vanish, this became the nominal solution strategy.

The arrival at Jupiter narrowly preceded conjunction, and consequently tracking data progressively grew noiser during the approach, although not in a uniform manner [4]. Use of a single accuracy for all the post-

release data (*i.e.* starting in August) was unreasonable, since variations in signal noise invited unwelcome amounts of subjectivity in choosing data weights, Instead, a pass-by-pros calculation of the data rms was made, from which a data weight was derived. By assuming that the power spectrum of solar plasma follows a Kolmogorov law for time scales larger than one day, [he rms was scaled to account for the sensitivity of doppler to diurnal changes. This method was iterative. In practice, data weights were scaled by a factor of 3.36 above the rms for nominal doppler. For some of [he data [his resulted in very small data weights, so a lower limit of 0.5 mm S"' was applied. Thus [he pass-by-pass weighting scheme resulted in a range of weights from 0.5 Mm S'[to 5 mm s^{-1}. This method returned consistency to the approach solutions and assurred that noisy passes would not unduly influence the results.

Near the end of November as conjunction approached, daily doppler biases (treated as uncorrelated stochastic parameters) were introduced as a means of accounting for [he increase in solar plasma density. The process noise was never more than 2.5 mhz (O. 17 mm s^{-1}), yet this method further improved the cons is tency of solutions.

New Jupiter Ephemeris

As the sensitivity to Jupiter's ephemeris grew, consistency in the OD solutions wavered again, but eventually settled down before [he final pre-lo data cutoff, The final reconstruction of the orbiter's approach using this data cutoff, labelled OL)1O5, represents our best estimate of the probe release / ODM events. Results for selected influential propulsive events occurring near [his time are listed in Table 2. This reconstruction also moved Jupiter nearly 2σ away from the latest (B 1950) JPI. ephemeris, DE-143. These corrections to the Jupiter ephemeris are listed in Table 3. As shown in Table 3, Jupiter's radial uncertainty improved by nearly 85% and the downtrack uncertainty by 67%. Without post-encounter data, Jupiter's out-of-plane (Normal) position improved only marginally.

Table 2. Selected Propulsive Events Near Probe Release

	A priori	Reconstruction	Uncertainty 1σ	Deviation
Spin-up for probe sep.	--	14,4 mms^{-1}	6.6 mms '	..
Probe separation	44,8 rams'	43.7 mms^{-1}	0.4 mms^{-1}	-2.5% (<1 σ)
Spin-down from sep.	..	8.4 mms^{-1}	7.7 mms^{-1}	--
Spin-up for ODM	--	1.6 mms"	13.0	mms^{-1} -
ODM AV	61.855 ms^{-1}	61.114 ms^{-1}	12 mm s"'	-1.2% (<1 σ)
00M *a*	101.890"	101.939"	0.021°	<1σ
ODM δ	'2'2.150°	2'2,096°	0.043°	<Icr
ODM avg. thrust	403,95 N	395.186 N	0.075 N	1σ
Spin-down from ODM	..	8.2 mms^{-1}	5.0 mms^{-1}	--

Table 3. Jupiter's Position Corrections with 1σ Uncertainty (wrt DE143)
Sun-centered Earth-Mean-Ecliptic of 1950, Jupiter-orbit Fixed
December 7, 1995 17:46 UTC SCET

Radial (km)	Downtrack (km)	Normal (km)
17.1 ± 1.4	-64.4 ± 11.3	74.2 ±179.1

Probe Trajectory Reconstruction

With an orbiter reconstruction, an updated Jupiter ephemeris, and (following probe playback) probe-entry telemetry, a probe reconstruction was possible. From the orbiter reconstruction, an epoch probe state

uncertainty and probe separation ΔV were deduced. From probe telemetry came [he actual time of entry from accelerometer data [51. This accumulation of information was sufficient to yield a trajectory and covariance mapped to the 450 km altitude entry conditions at Jupiter.

Error Sources

The major uncertainties in the probe trajectory included spacecraft state, Jupiter's ephemeris, probe separation ΔV, and probe spin-up ΔV. (Theoretically the probe spin-up ΔV equals zero since spin-up thruster pulsings should cancel translational movements; but [hey did not.) Furthermore, this residual ΔV was mainly constrained [o the direction perpendicular to the Earth-line, so little information was forthcoming from the tracking data. Even the probe separation event was highly uncertain because the error analysis of the release mechanism undertaken before launch was flawed. The analysis had been performed at room temperature, while the mechanism in the cold (shade) Of deep space was expected to respond 1.2% higher [6]. The mapping included solar pressure uncertainties as consider parameters, since they could not be estimated for the probe. All *a priori* uncertainties associated with these sources are listed in Appendix 1

Probe Entry

The probe's entry conditions for several OD solutions are listed along wirh the target and its 1σ tolerance in Table 4. (The requirements actually levied were stated in terms of 99%, or 2.6σ, uncertainty.) OD87 and TCM23 targetted the probe sufficiently close to the tin-get such that a second, planned targeting maneuver, TCM24, was cancelled. OD87, however, was a pre-separation solution and therefore the spin-up and probe separation uncertainties were considered. Following probe release and ODM, OD91 was computed to estimate the magnitudes of the spin-up and probe separation and their influence on [he entry parameters. Lastly, using the long arc, a complete probe reconstruction was performed. It shows that with respect [o [he targetted values, the probe arrived 18 seconds late (a 0.1σ miss), entered 0.23° too shallow (a 0.4σ miss) and 0.03° further south in latitude (a 0.2σ miss). These results are well within requirements.

Table 4. Probe Targeting History ±1σ
(JTED on Dec 5, 1995)

Delivery	Entry Time* (h:m:s)	Rel. Flight Path Angle (°)	Latitude (degrees)	Longitude (degrees)
Target ±1σ	22:04:26.0 ± 188 s	*-8.60 ± 0.55*	*6.5750.2*	none
We-release (OD87)	22:04:29.0 ± 37 s	-8.59 ± 0.15	6.57 ± 0.02	354.60 ± 0.46
Post-release (OD91)	22:04:04.5 ± 41 s	-8.31 ± 0.06	6.55 ± 0.01	355.61 ± 0.49
Reconstruction	22:04:43.9 ± 5.3 s	-8,37 ± 0.04	6.54 ± 0.01	354.79 ± 0.09

* on December 7 1995 (UTC)

Note that the pre-release entry time is closer to the reconstruction than the post-release solution. Probe release events apparently aliased into subsequent propulsive events (e.g. spin-down, ODM), thereby producing some spurious estimates for probe activities. Nevertheless the reconstructed entry time remains within 1σ of the post-release time, telling us that OD91 was aware of its potential to mislead.

Io Approach

Data Types

From late October to mid-November of the Jupiter approach, three optical navigation images (opnavs) were scheduled to supplement the radiometrics. These opnav data consisted of CCD images of Io, Europa, and Europa, against the stellar background. Navigation planning and much of the science activities at Io presumed a healthy spacecraft. A tape recorder anomaly on October 11 ultimately resulted in the loss of all opnav data, thereby disenfranchising the spacecraft of its target-relative navigation capabilities.

Predicted Performance

The post-ODM target for the orbiter was an Io closest approach altitude of 1000 km and 1.6° south latitude. Since perturbations to the spacecraft state, as well as uncertainties in the Jupiter ephemeris, could result in an altitude error of several hundred kilometers at the 1_0 flyby, four targetting maneuvers were planned from August through December. As it turned out, only one maneuver occurred. TCM26 delivered the spacecraft sufficiently close to the target -- leading to the eventual cancellation of all subsequent maneuver designs *(i.e.* TCM27,28,28A). Table 1 lists the maneuver times and salient events near the Jupiter encounter,

Predicted 1σ uncertainties in the Io B-plane for the approach maneuvers are listed in Table 5. Of the five maneuvers listed, only TCM26 and TCM29 (JOI) were performed. Owing to JOI's significance, the JOI maneuver delivery was designed only to update or "tweak" an extant nominal JOI design. Thus in Table 5, the JOI delivery refers to a parameter update, not to a complete maneuver design.

Table 5, Predicted Orbit Determination Uncertainties For 10 Delivery

Data Cut-Off Time (days)	Maneuver Supported	σB•R (km)	σB•T (km)	σLTOF (s)	Number of OPNAVS
10-114	TCM 26	±258	±395	±28.	0
IO-27	TCM 27	±64	±108	±8.1	1
IO-19	TCM 28	±60	±110	±8.3	1
10-6	TCM 28A	±32	±54	±4.1	3
10-3	JOI	±32	±26	±1.4	3

Io. Passage

The tape recorder anomaly forced the loss of science data at Io and was responsible for relaxing delivery requirements at Io. Camera pointing accuracies were no longer a concern; spacecraft energy change became the sole driver. Since the encounter was to occur at equatorial latitudes, this placed it very near the ecliptic, Thus the Io altitude was highly correlated with the B.T component of the B-plane, Energy change, proportional to flyby altitude, was therefore highly correlated with B.T. The B.R component was less important due to focussing effects.

For comparison with Table 5, Table 6 lists the degradation in the predicted uncertainties that accompanied the loss Of opnav data. Surprisingly, in the last week of the approach, the real OD (lacking opnavs) produced smaller uncertainties in B.T than were predicted in the simulation with opnavs. This was a consequence of consider effects.

In general, the B.T component can be extracted from a tracking signal over a period of several days. And as the spacecraft nears a planet this information begins to yield significant improvements to B•T and time-of-flight. The out-of-trajectory-plane component (B•R) can only be extracted from the observed signal over a period of several weeks, all else equal. Hence B.R knowledge improves only marginally with doppler, although it can be improved with opnav data. The B.R component for Galileo, as seen in Table 6, remained large because of the opnav losses,

The movement of the spacecraft in the B-plane during approach is illustrated in Table 6 and Fig. 1, Note that the altitude remained within approximately ±100 km of the 1000 km target during the month preceding the encounter.

The ≈100 km altitude en or was (apparently) acceptable to the Galileo project due to arrival options at Ganymede, in June 1996. Moreover from a mangagement perspective, the low altitudes predicted by OD96

and OD97P2, combined with the *nominal* JOI, produced *a* bonus. The additional AV imparted to the orbiter by the low flyby was seen to (serendipitously) advance the arrival date at Ganymede very nearly one Ganymede orbital period (1 week). Thus the orbiter could remain on its "low" trajectory [thereby eliminating last-minute sequence parameter changes), perform the *nominal* JOI burn ([hereby eliminating Imt-minute main engine parameter changes), reach Ganymede with a subsequent nearly-nominal sequence of events, and yet still remain within [he orbiter's budgetted propellant allotment.

Table 6. 10 B-plane History with 1σ Uncertainties (EMO50)
(No Opnavs)

Data Cut-Off Time (days)		Maneuver Supported	5*R (km)	B•T (km)	TCA' (h:m:s)	Altitude (km)
Target			87	2847	17:45:44	1000
IO-114	(0091)	TCM 26	433 ± 373	925 ± 437	41:55 ± 29	-800 ± 429
Io-27	(OD94)	TCM 27	205 ± 120	2925:131	45:39± 11	1084 ±126
10-19	(OD95)	TCM 28	226 ± 102	2919 ±149	45:40± 12	1080 ±145
10-6	(OD96)	TCM 28A	420 ± 70	2753134	45:53 :-2.1	937 ± 36
10-3	(OD97P2)	JO I	392 ± 71	2708 ± 23	46:58 ±0.8	888 ± 27
Io+0.01	(OD100)	--	474 ± 2	2699 ± 2	47:00 ±0.1	892 ± 2
Io+55	(Recon.)	--	469 :0,2	2708 ±0.2	47:00 :0,0	900 ± 0.3

* on December 7 1995 (UTC)

A Posteriori Performance

The 10 flyby reconstruction is presented here. In [his analysis realistic and adequate constraints have been established by applying the following procedures. 1. Firmly restraining both Io inbound and outbound asymptotes (with [en weeks of F1 and H), 2. adjusting data weights uniquely pass-b-v-pass. 3. eschewing unmodellable data, and 4. applying the latest models to the problem (see Appendix 2).

The Reconstruction Data Set

November 21 was selected as the epoch of the reconstruction data set since that date corresponded [o the longest interval before Io without any propulsive events located in-between. January 31 was chosen as the end of the arc because that point on the trajectory was regarded sufficiently far from Jupiter. Moreover these bounds also provided about ten days of nominal (low rms) doppler at each end of the arc -- sufficient. to establish both the inbound and outbound asymptotes with high degrees of certainty. (Most Of the intervening F2 was noisier due [o solar conjunction.) To illustrate, the first ten days of doppler on the inbound side exhibited an rms scatter of 6.9 mhz, or 0.5 mms^{-1} across [his interval. Thus control of the inbound asymptote was established with the following asymptotic uncertainties: S•Rσ = 56 μrad. S•Tσ = 3 μrad. Similar values existed for the outbound asymptote.

Fig 1 here

Noncoherent Doppler

Io Residuals

One-way incoherent doppler tracking around the Io encounter admitted an immediate reconstruction of the flyby conditions. Three days of F1 were included in the data set, from Dec. 5 to Dec. 8 (coherent data was unavailable from Dec. 7, 4:16 UTC SCET through Dec. 8, 7:24). Since F1 data is based on [he frequency stability of the ultra stable oscillator (USO), the changes in F1 characteristics were correlated to fluence effects on the USO. This fluence originated in the Jovian radiation belts and Io torus. These regions were poorly characterized (indeed, as was the solar corona), yet transmissions from [he orbiter propagated through all three regions.

Several fluence models were constructed, but in the end all were found wanting or impractical. The criteria we applied to adjudicate the pan-Io F1 was informal. The F1 residuals were measured visually against a "trusted" trajectory. If the dara developed unaccountable trends or discontinuities, wc attributed such behavior to radiation impingement. Exactly this behavior is illustrated in Figure 2. The residuals fall off rapidly after 19:42, as indicated, and the data after that time were deleted. In contrast, data before 19:42 remained remarkably stable. These F1 (before 19:42) were assigned unique per-pass *a priori* weights between 20 and 60 mhz (3 to 9 mm s^{-1}). For comparison, the *postfit* rms residuals showed a spread of 13 to 22 mhz.

Fig 2 here

JO I Residuals

As in the Io flyby, the JOI reconstruction was limited by the availability of only F1 and adequate modelling of the radiation zones. Nevertheless the F1 could bound discrete events and esti mate the dur ation of JOI. For this reason two hours of F1 during JOI were included in the reconstruction set. Because the data quality was poor and data models nonexistent during this period, the *a priori* F 1 was de-weighted to 150 mhz (20 mm s^{-1}). After solving for JOI. the postfit F1 rms residuals fell to 31 mhz (4 mm s^{-1}), indicating that the initial weighting was conservative.

Coherent Doppler

The majority of the data set consisted of two-way coherent doppler, spanning November 21 to January' 31, 1996, These data were assigned per-pass *a priori* uncertainties between 7 and 70 mhz (0.5 [o 5 mm s^{-1}), with the mode being about 30 mhz. (I'his range of weights excludes the first F2 pass following JOI on Dec. 9, which because of its proximity to conj unction was de-weighted to approximately 15 mm s^{-1}.) Solar conjunction on December 19 imposed a data black-out from December 10 to December 28 (-7° to +7° Sun-Earth-orbiter angle). Moreover for approximately three or four days on each side of this gap, significantly larger residuals were evident. The residuals straddling this conjunction gap were initially assigned a weight of 60 mhz. The postfit rms of these data dropped marginally to ≈55 mhz, or ~4 mm s^{-1}. (This degradation derived from propagation *of* orbiter transmissions through the solar corona.) As seen in Fig 3, the F2 residuals. the data improves markedly beyond the intermediate region.

Preliminary Io Reconstruction

A preliminary Io reconstruction was attempted on the day of [he flyby with 20 minutes of post-lo data. This solution was la belled OD100 and is listed in 'I'able 6. A comprehensive exposition of reconstructed values will be detailed in the following section; this section exists merely to point out the accuracy of OD100. a solution produced quickly with minimal modelling, and from minimal post-encounter date.

OD100 calculated the closest approach altitude to equal *8922 2* km. The mass of Io (GM_{Io}) was estimated at $5959.8 \pm 0.9\ km^3 s^{-2}$. These determinations can be compared with values computed from the long arc reconstruction (discussed next): 900 ± 0.3 km anti $59615 \pm 0.2\ km^3 s^{-2}$ respectively. The agreement is good considering the minimal level of modelling used in [his solution. We should drop this section.

Fig 3 here

Rigorous Io/JOI Reconstruction

The long arc 10 reconstruction applied greater rigor than the preliminary reconstruction. The long arc contained four times as much data and employed improved Io and Jupiter ephemerides, and estimated the Io gravity field.

A list of all estimated and considered parameters in the long arc Io reconstruction is supplied in Appendix 2. The estimated quantities included orbiter state, satellite ephemerides, satellite masses (as well as the second order gravity field of Io), Jupiter's mass, Jupiter's J_2 and J_4 harmonic terms, Jupiter's pole orientation. spacecraft propulsive events including JOI (where the thrust was modelled with a 5th degree polynomial and an exponentially decaying acceleration), solar pressure, and F1 bias, drift, and drift-rate terms. (Stochastic

F2 biases and ionospheric processes were demonstrated elsewhere to be inconsequential to the Io reconstruction. so they were not included here.) As previously noted, F2 residuals from the converged solution are shown in Fig. 3.

Io Ephemeris

The orbiter's encounter with Io provided an unprecedented opportunity [o directly measure the location of Io relative to Earth. (The Io-spacecraft relative measurement was 540x more sensitive than Voyager.) By also measuring the Jupiter-spacecraft relative state, 10's location with respect m Jupiter may then be interred This measurement was obtained by radiometric means during the flyby. The measurement indicated an error in Io's Jovi-centric state at [he time of the flyby of the following magnitude: 9 km and 2 ms^{-1} (RSS), with respect to the JPL satellite ephemeris JUP076.

A priori state knowledge of Io was represented by JUP076. Usin g that extant ephemeris as a reference, component differences between it and the updated Io ephemeris could be computed; they are presented as plots in Fig. 4a, b.c. (The plots have a jagged appearance due [o the discretization of the plotting program.) The greatest difference (uncertainty) between JUP076 and the reconstructed 10 ephemeris exists in the out-of-plane direction (the differences oscillate over onc orbital period from approximately -50 to +50 km, a little more than 1 *a priori* σ). This was expected, as that direction represe nts the greatest uncertainty in the Io ephemeris. The downtrack difference varies between 0 and 20 km, The mean of this latter difference implies a downtrack secular bias of about 10 km in JUP076. That in turn suggests a mean motion error in Io's ephemeris. Radial differences are seen [o oscillate between -5 and 5 km. The changes indicated by these plots are small and not really significant. as they lie within approximately 1σ of JUP076. (For comparison, Appendix 2 lists the JUP076 u *priori* state uncertainties .)

Europa Ephemeris

Similarly, new insights were forthcoming at Europa, as the flyby provided data 40x more sensitive than Voyager. An equivalent satellite state measure ment was also obtained for Europa, and an adjustment in its Jovi-centric state was computed: 108 km and 3 ms^{-1} (RSS). Plots of the differences between the updated Europa ephemeris and JUP076 are given in Fig. 5a, b, c. The downtrack error dominates [he Europa ephemeris because of the approximately 40 km bias (about 1σ) *seen* in Fig. 5b. (This is indicative of a mean motion error'.) The out-of-plane differences are significantly larger (≈200 km), but the mean dots no: show a deterministic offset. These out-of-plane (and radial) *differences* oscillating around zero indicate a small adjustment to the node has occurred,

The changes for Europa are significantly larger than those for Io and may indicate that 10, with the highest orbital frequency of the four Galilean satellites, has the best determined *a priori* ephemeris of the four 1[follows that disagreements between the updated ephemerides of Ganymede (and Callisto) and JUP076 may show even greater degradation as Galileo visits those satellites in turn.

Figs 4 and 5 here

Io Gravity Field

The present work also presents preliminary results from the first-ever sampling of the Io gravity field. The following parameters were estimated for the Io gravity field: mass (GM_{Io}), J_2, and C_{22} (the solution exhibited no sensitivity to S_{22}).

The details of this gravity field determination are outlined below. A sample space was constructed from seven parametric trials. Each trial adjusted one of the following parameters: arc length, *a priori* uncertainty in J_2 and/or C_{22}, or correlation between *a priori* J_2 and C_{22}. See Table 7.

Arc length was subdivided into three distinct data sets. The term 'long arc' (already mentioned) denotes the entire data set, from Nov. 21 to Jan. 31. Similarly. 'intermediate arc' will refer to a data arc from Nov. 21 to Dec. 7 19:42 UTC (*i.e.* to one and one-quarter hours past Io closest approach). The 'short arc' began on Dec. 3 18:00 and ended at the same time as the 'intermediate arc', Dec. 7 19:42.

A priori J_2 and C_{22} uncertainties were assigned one of two values: nominal (derived from a layered, hydrostatically -equilibrated model for 10), or unconstrained. Guided then by the Io model, nominal uncertainties were given the following proportions: J_2 ±31%, C_{22} ±12%. The unconstrained uncertainties were left wide-open: J_2 ± 500%, C_{22} ±1600%. The J_2 and C_{22} coefficients were *uncorrelated for most* trials. For a hydrostatic body in synchronous rotation, however, some theorists have argued for a constrained coupling between J_2 and C_{22}[7]. By employing such a theoretical device, the proportional correlated uncertainties can be shown to be: J_2 ±.167% and C_{22} ± 167% (plus cross -terms). This particular case is listed as Trial 3 in Table 7.

In Table 7, Trial 1 represents the nominal long arc solution. (The residuals shown in Fig. 3 were a product of this solution.) Trial 2 represents the case without any a *priori* constrains on J_2 and C_{22}. GM_{Io} falls, but J_2, C_{22} and GM_{Jup} all rise with respect to the nominal in this latter trial, although not significantly (except C_{22}). Trial 2 in effect establishes bounds on the movements of J_2 and C_{22}, but is nor representative of reality because of the unnaturally large sigmas placed on the harmonics. Nevertheless, it is comforting to note that this solution closely approximates Trial 1. The uncertainty on GM_{Jup} for Trials 1 and 2 is slightly larger than their *a priori* sigmas because of consider effects -- primarily the ionosphere.

Table 7. 10 Gravity

Trial	Flyby Alt. (km)	Latitude (degrees)	TCA (m:s)	J_2 x 10^{-6}	C_{22} x 10^{-6}	GM_{Io} (km^3 s^{-2})	GM_{Jup} (km^3 S^{-2})	o Adjust. (km RSS)
1	900.4±0.3	-9.60 ±0.01	47:0010.01	2044? 454	1591±31	5961.5±0.2	126712811± 102	9
2	900.5±0.4	-9.63 ±0.01	47:00 tool	2202'.672	2608± 34	5961.0±0.2	1267128191102	8
3	898.1±0.5	-9,5610.02	46:59 ±0.01	8607:114	2582-'-34	5960.6±0.2	1267127901 8	DNC
4	900.4±0.3	-9.60 ±0.01	47:00:0,01	2398? 597	1535131	5961.5±0.2	126712770± 100	5
5	899.9±0.7	-9.55 ±0.02	46:59:0.01	1037*554	600	5961,950.2	126712764± 100	6
6	901.2? 0.7	-9.52 ±0.01	46:59 ±0.00	o	0	5961.9±0.2	126712764± 100	5
7	887.4±0.3	-9.59 ±0.01	46:59 ±0.01	1879± 599	536±31	5960.4?0.3	126712827± 13	27

Legend

Trial	Data Arc	Notes	apriori J_2 x 10^{-6}	apriori C_{22} x 10^{-6}
1	Nov21-Jan31	70 day arc, uncorrelated J_2 and C_{22}	2000 ± 610	600170
2	Nov21 - Jan 31	70 day arc, uncorrelated, "free" J, and C_{22}	2000 ±10,000	600 ±10,000
3	Nov21 - Jan 31	70 day arc, correlated J, and C_{22}	2000 ± 3333	600 ±1000
4	Nov 21 -Dee 7, 19:42	16 day arc, uncorrelated J_2 and C_{22}	2000 ± 610	600 ±70
5	Nov21-Dec7, 19:42	16 day arc, estimate J_2 only	2000 ± 610	600
6	Nov21 - Dec 7, 19:42	16 day arc, did not model J_2 nor C_{22}	o	0
7	Dec 3- Dec 7, 19:42	4 day arc, uncorrelated J_2 and C_{22}	2000 ±61O	600:70

Trial 3 represents the correlated J_2 and C_{22} case. This attempted solution did not converge. The filter was incapable of fitting the correlated Io gravity model to the pre- and post-Io data arcs. Lack of convergence indicates a severe modelling error, and we are forced to conclude that a hydrostatically -induced correlation between J_2 and C_{22} does not exist within Io. The values tabulated for Trial 3 were extracted from the (unconverged) 34th iteration.

Trial 4 is the intermediate analog to Trial 1, The intermediate arc was introduced with the intention of removing possible unmodelled error sources from the post-Io trajectory. As seen in Table 7, the gravity

solutions for Trials 1 and 4 are remarkably similar. The largest discrepancy is a 4 km difference in the position of Io. But we expected a poor determination of Io's position with the intermediate arc since the out-bound trajectory in Trial 4 is poorly defined. Thus mis-modellings in the post-Io trajectory are either non-existent or insignificant.

Trial 5 examined [he possibility that C_{22} was masking J_2. Thus C_{22} was fixed in this trial. In the absence of other data Trial 5 might represent a valid solution. Examination of the residuals from this solution shows, however, a poor fit to [he encounter data. Thus Trial 5 is not a satisfactory solution. Trial 6 is the null case -- neither J_2 nor C_{22} were modelled. While this is an unsatisfactory model, it provides a useful comparison [o other trials. Residuals for this trial are illustrated in Fig. 6. Clearly the solution is mis-modelled. The residual signature at closest approach has a scatter of 280 mhz, with an overall rms of 33 mhz for the data shown.

Fig 6 here

The salient item to note from these analyses is the consistency of the uncorrelated long and intermediate arcs, Trials 1 and 4, compared with the inconsistency of the remaining trials. For Trials I and 4, J_2 varies between 2.0×10^{-3} and 2.4×10^{-3} with an uncertainty of about $\pm 0.5 \times 10^{-3}$. C_{22} solves out slightly smaller, with a value of about 1.5×10^{-3} and an uncertainty of $\pm 0.03 \times 10^{-3}$. Some mis-modelling nevertheless remains in the Io gravity field, as demonstrated with the Io residual plot from Trial 1 in Fig. 7.

To determine the level of significance of the signature in Fig. 7.0 comparison was made with the null case in Fig. 6. The peak-to-peak range in Fig. 6 is roughly twice the range of the residuals seen in Fig. 7. The overall data rms for Fig. 7 is 24 mhz -- approximately 70% of Fig. 6. Thus modelling J_2 and C_{22} has improved the fit, although the influence of Io harmonics o n gross features (GM_{Io}, flyby altitude) is minimal. In any event, a gravity signature persists near closest approach for Trials I - 6.

Fig 7 here

The short arc, Trial 7, reproduces the method of Anderson et al [8]. Trial 7 moreover. succeeded in eliminating [he closest approach gravity signature. See Fig. 8. "Flat" residuals therefore could be achieved, but at great expense, as demonstrated by adding more data. To wit. returning to the long arc solution and incorporating: the Io gravity parameters from Trial 7 into that analysis leads to inconsistent results. The solution exhibited numerous local minima and would not converge. That is, the gravity field determined for Io from the short arc would, in turn, yield a trajectory in strong disagreement with the long arc asymptotic values.

The Trial 7 values in Table 7 starkly contrast with all previous trials. In particular, the altitude is appreciably lower, and the shift of 27 km (and $0.8\ ms^{-1}$) in 10's state is very significant compared to Trials 1 -6. The largest components of this change were 23 kilometers along the out-of-plane axis and -68 cm s^{-1} in the radial direction. The largest component adjustments for the long arc were 7 kilometers and $2\ ms^{-1}$, both in the. out-of-plane direction.

Fig 8 here

The trade for position adjustment rather than velocity observed in Trial 7 is the expected exchange when spacecraft state is poorly determined from a dearth of tracking data. The short arc, apparently, could not exert sufficient control over the inbound asymptote -- leaving the spacecraft state unconstrained. Io was [hen free to move within the bounds of its covariance since [he spacecraft did not establish any limits. Hence both states were adjusted until the least-mean squares filter removed the only remaining bump -- the gravity signature. A comparison between the asymptotes of the long arc and short arc clearly shows this. The inbound asymptotic uncertainties of the short arc are significantly larger compared to the long arc: $S \cdot R\sigma \simeq 85$ µrad, $S \cdot T\sigma \simeq 5$ µrad, $V_\infty \sigma = 84\ ms^{-1}$ v, S*RO = 56 µrad, $S \cdot T\sigma \simeq 3$ µrad, $V_\infty \sigma$. 71 ms^{-1}, respectively, .4s a manifestation of these uncertainties. [he respective trajectories on Dec. 318:00 (epoch for Trial 7) differed by 49 km and 19 cm s^{-1} (RSS), while the altitude difference at closest approach was 3 kilometers (all in Jupiter-centered coordinates). The two trajectories bear little resemblance to one another. and similarly yield analogous conflicts regarding the 10 gravity field.

We conclude that the best estimate for the Io gravity field at this time is from the long arc solution. This solution gives GM_{Io} = 5961.5 ± 0.2 $km^3 s^{-2}$, $J_2 = 2044 \pm 454 \times 10^{-6}$, $C_{22} = 1591 \pm 31 \times 10^{-6}$, and $S_{22} = 0 \pm 70 \times 10^{-6}$. The observations also indicate that a gravity model of Io containing only second order terms is an inadequate representation of the field. Future improvements to the satellite ephemerides in general will improve this Io reconstruction by establishing tighter limits on Io's covariance.

JOI Reconstruction This part still needs work

The JOI model consisted of the following parameters: JOI start time, JOI duration, burn direction (α, δ), and thrust (modelled with a fifth degree polynomial). The nominal thrust profile of JOI is illustrated in Fig. 9. Since a fifth degree polynomial cannot, in general, adequately fit a curve of the shape illustrated in Fig. 9, an exponentially decaying acceleration of five minute duration was independently estimated during the first five minutes of JOI to supplement the JOI thrust model during that time. Additionally, the spire up and spin-down activities occurring on either side of JOI were modelled with impulsive burns (instantaneous AV components along three orthogonal axes). Table 8 lists the reconstructed values and uncertainties of JO1, as well as their movement from the associated nominal values. The JO I ΔV estimate determined an overburn of 0.1 %, with spacecraft pointing in error by approximately the same proportion (0. 1%). Note that right ascension, JOI start time, and JOI duration all exhibit multi-σ shifts from their nominal values. Fig 9 here

Table 8. JO I Events

	Magnitude	Uncertainly 1σ	Deviation
Δv	645,301 MS '??	0.200 ???	+ 0.13% (<1σ)
α	87.765'	0.0063	2.8 σ
δ	27,609°	0,024	<1 σ
start time	00:27:22.0 UTC	0.2 s	-00:00:02.4 (2σ)
duration	49 m 4.4s	0.3 s	+27.3 s (5σ)
avg. thrust	392.8 N???	0.3	<1 σ
spin-up	6.64 cm s"'	2.37	
spin-down	2.93 cm s"'	2.06	

Jupiter Gravity Field

A determination of a subset of Jupiter's gravity parameters and its pole orientation *i.e.* GM_{Jup}, J_2, J_4, and (α, δ), are presented here.

The Jupiter GM is estimated ro equal 126,712,811 ± 102 $km^3 s^{-2}$ -- a value within the uncertainty quoted by Campbell and Synnott [9]. The solved values of J_2 and J_4 do not differ from values in the literature. The pole direction of Jupiter, however, undergoes a significant change, The right ascension moves by 0.028", a change of nearly 2σ. The declination moves -0,0025°, a shift of 1σ. The updated values and uncertainties are listed in Table 9.

Table 9. Jupiter Gravity (E MO50)

GM_{Jup} ($km^3 s^{-2}$)	J_2 x 10^4	J_4 x 10^{-6}	α (degrees)	δ (degrees)
126,712,811 ±102	14,736 ± 3	-587 ± 15	268.027 ± 0.007	64.502 ± 0.002

REFERENCES

1. L. A. D'Amario, D.V Byrnes, R.J. Haw, W. E. Kirhofer, F. T. Nicholson, M.G. Wilson, "Navigation Strategy For [he Galileo Jupiter Encounter and Orbital Tour," AAS/AIAA Astrodynamics Specialist Conference, Halifax N. S., August 14-17 1995.

2. P.G. Antreasian, F.T. Nicholson. P.H. Kallemeyn. S. Bhaskaran, R.J. Haw, P. Halamek, "Galileo Orbit Determination for [he Ida Encounter," AAS Paper 94-132. AAS/AIAA Astrodynamics Conference. Cocoa Beach, FL, February 14- 16, 1994.

3. W'. J. O'Neil, N. E. Ausman, M. R. Landano, R. T. Mitchell, and R. J. Reichert, "Galileo Preparing for Jupiter Arrival", Paper IA F-94.Q.5.355, presented at the 45th Congress of the International Astronautical Federation, Jerusalem. Israel, October 9-1-1. 1994.

4. R. Woo, J.W. Armstrong, M.K. Bird, M. Patzold, "Fine-5cnlc Filamentary Structure in Coronal Streamers", The Astrophysical Journal, 449:L9 1-194, August 10, 1995.

4?. R. Gershman, "Galileo Mission Requirements Document", JPL, PD625-51, Rev. E, March 1987

5. C.K. So beck, "Galileo Probe Entry Time -- Revision 1", NASA Facsimile Transmission to Pat Melia, April 3, 1996.

6. D. Carlock, "Effect of Spring Temperature on Probe Separation Velocity", Hughes Aircraft Corp. Document HS373-0045-0070, December 5, 1994.

7. G. Schubert, private communication, December, 1995.

8. J. D. Anderson et al, "Io Gravity," Science, May 3, 1996. incomplete citation

9. J.K Campbell, S. P. Synnott, "Gravity Field of the Jovian System From Pioneer and Voyager Tracking Data", The Astronomical Journal, Volume 90, Number 2, pp. 364-372, February 1985.

APPENDIX 1

A PRIORI Model Uncertainties
Jupiter Ephemeris Determination

Estimated Parameters	Standard Deviation (1σ)	Comments
State	10,000 km 10,000 kms^{-1}	(X, y, z) (dx, dy, dz)
TCM 23,26	1% of ΔV (each component)	impulsive maneuvers
Radial acceleration	5 x 10^{-13} kms^{-2} axial	
ODM thrust	8.4 N	2 %
a	O.1O°	loose
δ	0.1O°	loose
Attitude corrections (SIturns)	2 mms ' spherical	
Line flushings (RPMs)	1 mms^{-1} axial, 0,7 mms^{-1} lateral	
Probe separation ΔV	0.6 rnms ' axial, 2,3 mms ' lateral	
Spins-up / down	10 mms ' axial, 16 mms^{-1} lateral	
Solar pressure	10%	specular & diffuse components
F2 bias	≈2.5 mhz	stochastic parameter[1]
Ionosphere zenith delay (day)	75 cm	stochastic parameter'
Jupiter ephemeris		DE143
radial	9.4 km, 0.6 mm s '	
downtrack	34.3 km, 0.1 mm s"	
out-of-plane	229.0 km, 1.6 mm s '	

Considered Parameters	Standard Deviation (1σ)	Comments
Troposphere zenith delay	1 cm dry, 4 cm wet	
Ionosphere zenith delay (night)	15cm	
DSN station locations (R, L, Z)	50 cm, 70 cm, 6 m	
Earth ephemeris		
radial state	7 m, 0.2 mm s"'	
downtrack state	1,0 km, 0,002 mm s"'	
out-of-plane state	1.7 km, 0.3 mm s"'	
10 ephemeris		revised JUP071
radial state	18 km, 300 cm s'	average over 1 orbit
downtrack state	81 km, 69 cm s"'	average over 1 orbit
out-of-plane state	63 km, 230 cm s'	average over 1 orbit
10 mass (GM)	14 km' s"'	revised JUP071
Europa mass (GM)	13 km^3 s"'	revised JUP071
Jupiter mass (GM)	309 km^3 s"*	revised JUP071
J_2	3.0 x 10^{-6}	
J,	15.4X 10^{4}	
Jupiter pole (a, δ)	(0.001 8°, 0.0008°)	

R, L, Z = spin radius, longitude, distance from equator parallel to polar axis

1. data batch length = single tracking pass, correlation time = O days *(i.e.* white noise)

APPENDIX 2

A PRIORI Model Uncertainties
Io / Europa Ephemeris Determination

Estimated Parameters	Standard Deviation (1σ)	Comments
State	2000 km 100 ms^{-1}	(x, y, z) (dx, dy, dz)
JOI thrust	8.4 N, 10^{-3} N s^{-1}, $7x10^{-4}$ N s^{-2}	5th degree polynomial (n. 2,3,4)
JOI a	*0.023°*	
JOI δ	*0,023°*	
JOI start time	I s	
JOI duration	5 s	j min duration
JOI exponential acceleration	$2 x 10^{-6}$ kms^{-2} axial, $1 x 10^{-11}$ kms^{-2} lateral	
JOI exponential accel time const	10 s“	
Spins-up/down	10 mms^{-1} axial, 16 mms' lateral	
Solar pressure	1 o%	diffuse component only
Attitude corrections (SIturns)	2 mms ‘ spherical	
Line flushings (RPMs)	1 mms ‘ axial, 0.7 mms ‘ lateral	
Io ephemeris		revised JUP076
radial state	6 km, 18 cm s^{-1}	
downtrack state	45 km, 49 cm s“'	
out-of-plane state	36 km, 112 cm s^{-1}	revised JUP076
Io mass (GM)	10 $km^3 S^{-2}$	
Io J_2	61 OX1O”	
Io C_{22}	$70 x 10^{-6}$	
Io S_{22}	70 X104	revised JUP076
Europa ephemeris		
radial state	7 km, 16 cm s“	
downtrack state	50 km, 28 cm s‘	
out-of-plane state	69 km, 161 cm s^{-1}	revised JUP076
Europa mass (GM)	10 km' s“'	revised JUP076
Jupiter mass (GM)	100 $km^3 S^{-2}$	
Jupiter J_2	$3.0 x 10^{-6}$	
Jupiter J_4	15.0 X104	
Jupiter pole (α, δ)	(0.015', 0.003°)	
F1 bias	10 hz	(4 batches over 3 days, for 10&
F1 bias rate	1 mhz s“'	1 batch over 2 hours, for JOI)
F1 bias acceleration	0.02 μhz s^{-2}	

Considered Parameters	Standard Deviation (1σ)	Comments
Ionospheric zenith delay	75 cm day, 15 cm night	
Earth ephemeris		
radial state	7 m, 0.2 mm s^{-1}	
downtrack state	1.0 km, 0.002 mm s“'	
out-of-plane state	1.7 km, 0.3 mm s“'	
Jupiter ephemeris		from reconstruction

radial state	1.4 km, 0.2 mm s ‘
downtrack state	11.3 km, 0.03 mm s ‘
out-of-plane state	179,1 km, 1.2 mm s

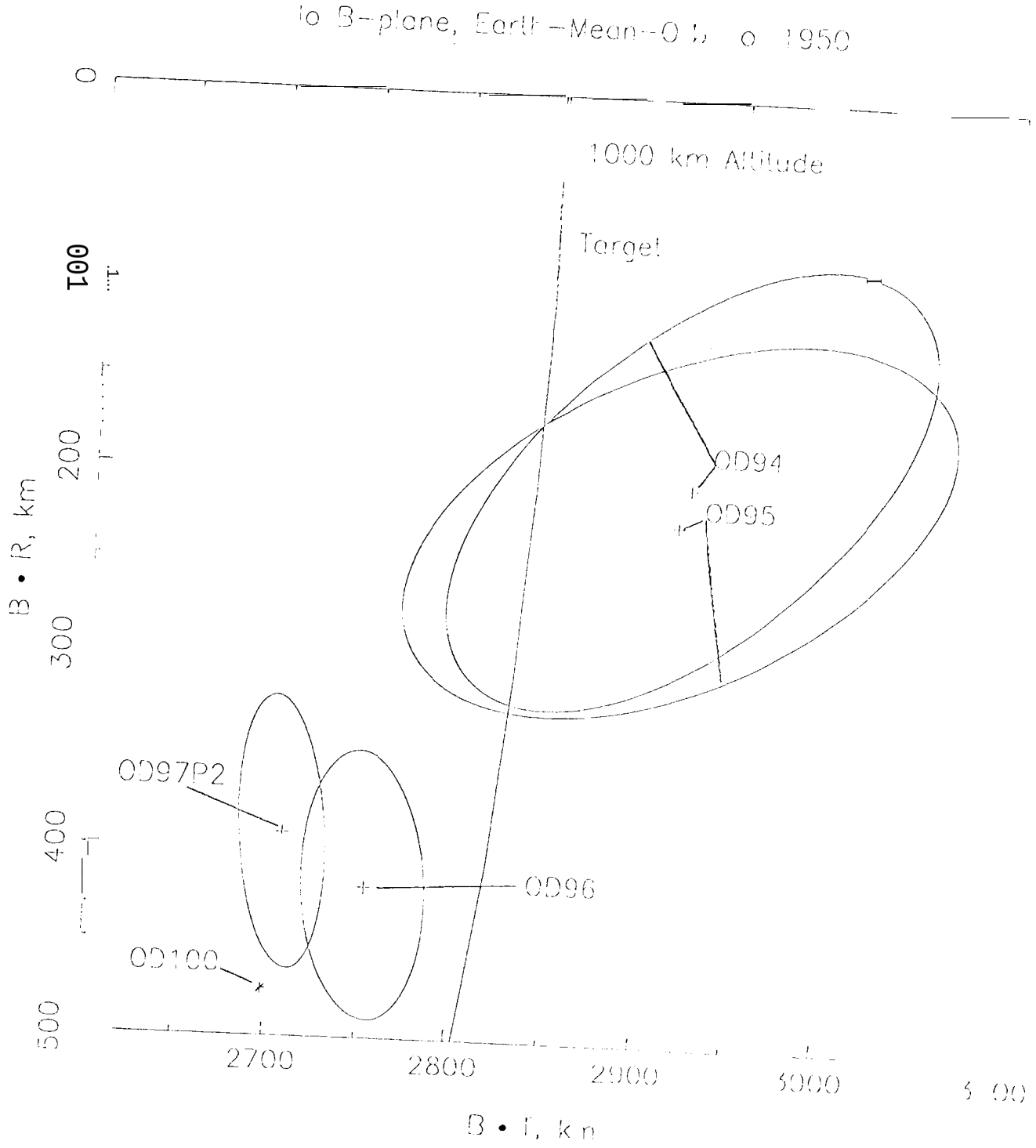
Io B-plane, Earth-Mean-O
1000 km Altitude
Target
OD94
OD95
OD97P2
OD96
OD100
B • R, km
B • T, km
100
200
300
400
500
2700
2800
2900
3000

FIG. 4.1

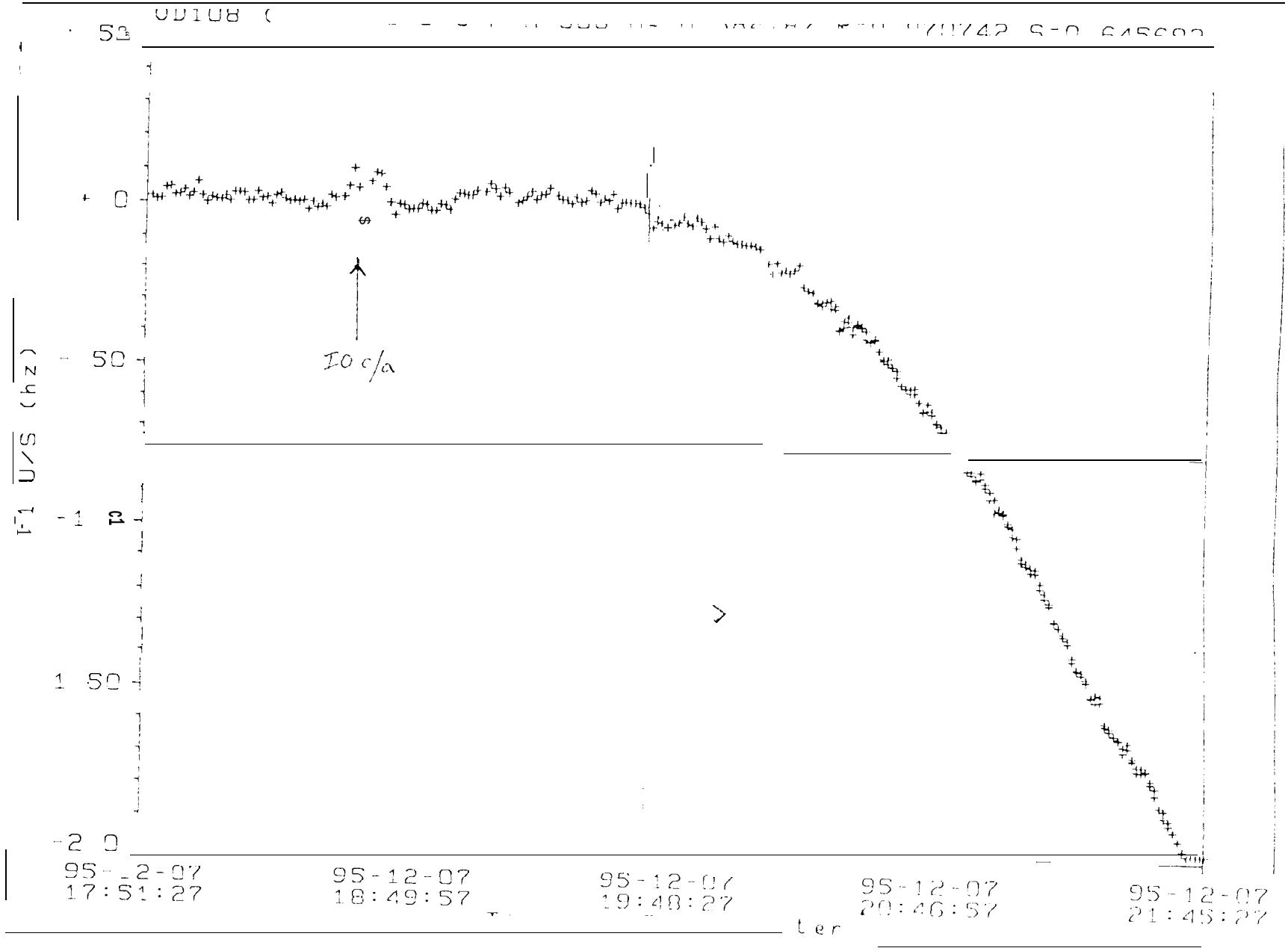
50
0
50
-1 1
50
-2 0
I-1 U/S (hz)
Io c/a
95-12-07
17:51:27
95-12-07
18:49:57
95-12-07
19:48:27
95-12-07
20:46:57
95-12-07
21:45:27

FIG. ~~1~~ 2

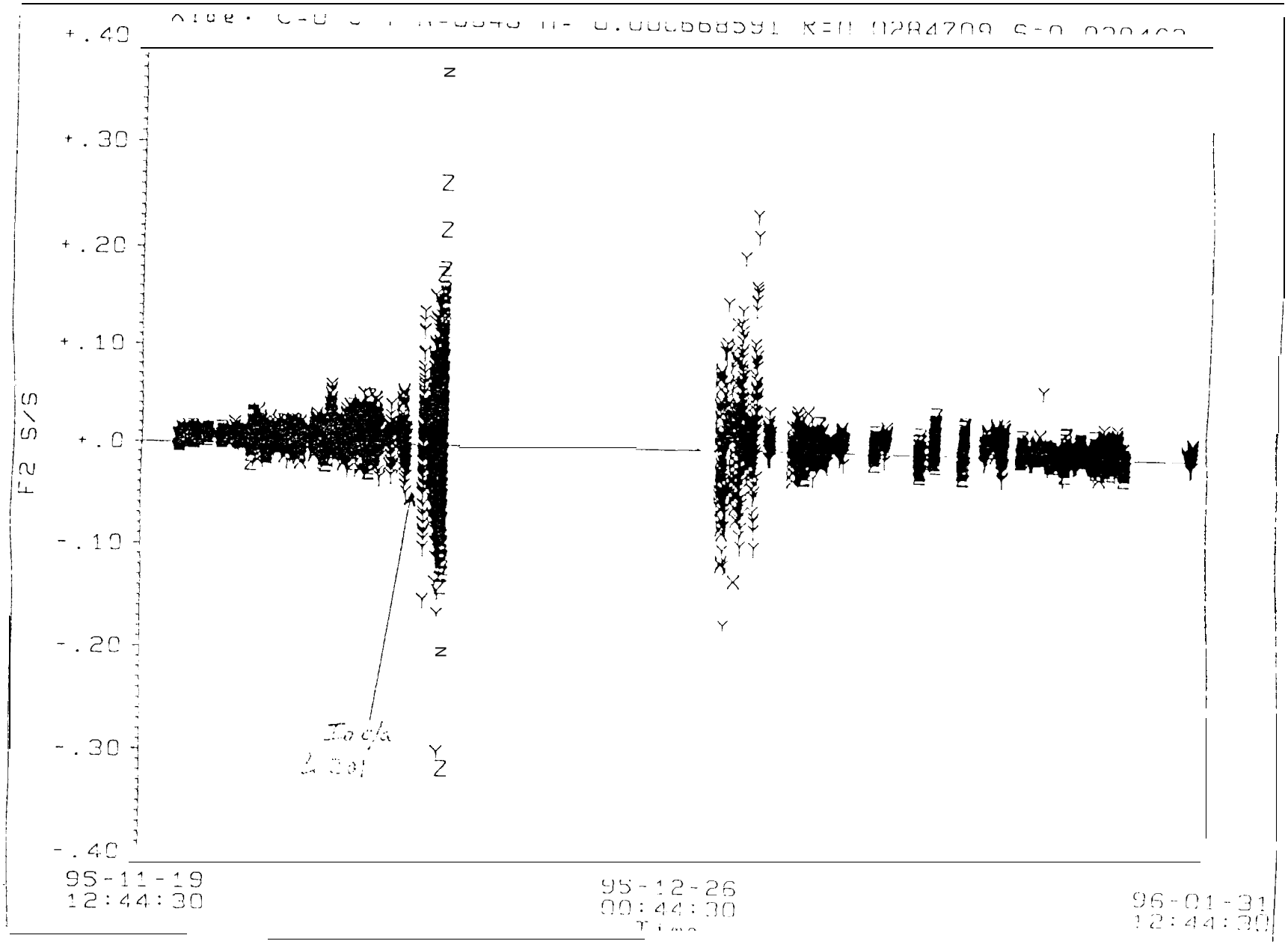
+.40
+.30
+.20
+.10
+.0
-.10
-.20
-.30
-.40
F2 S/S
95-11-19
12:44:30
95-12-26
00:44:30
96-01-31
12:44:30

FIG. ~~2~~ 3

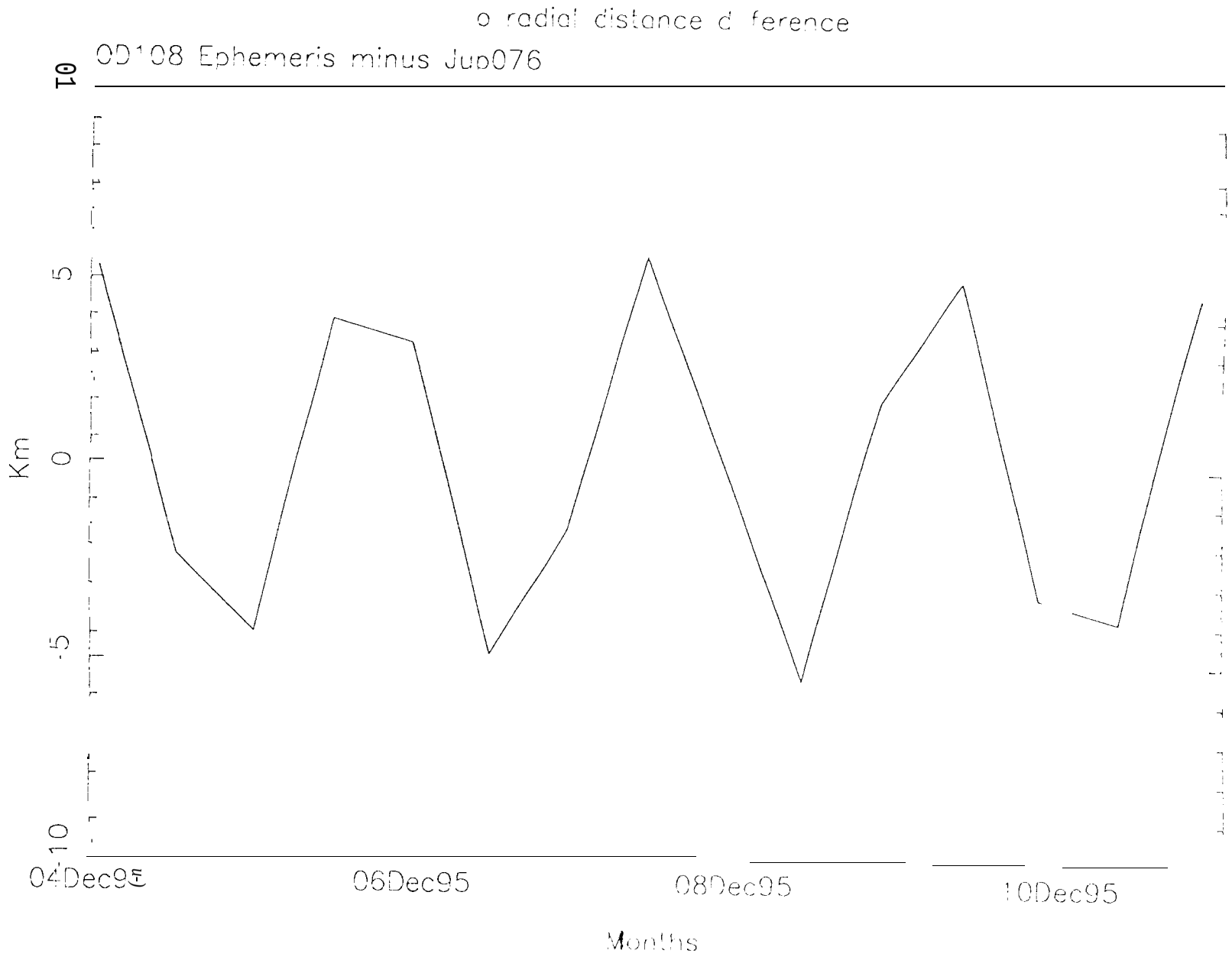
o radial distance d ference
OD108 Ephemeris minus Jup076
01
Km
5
0
-5
10
04Dec95
06Dec95
08Dec95
10Dec95
Months

FIG ~~3a~~ 4a

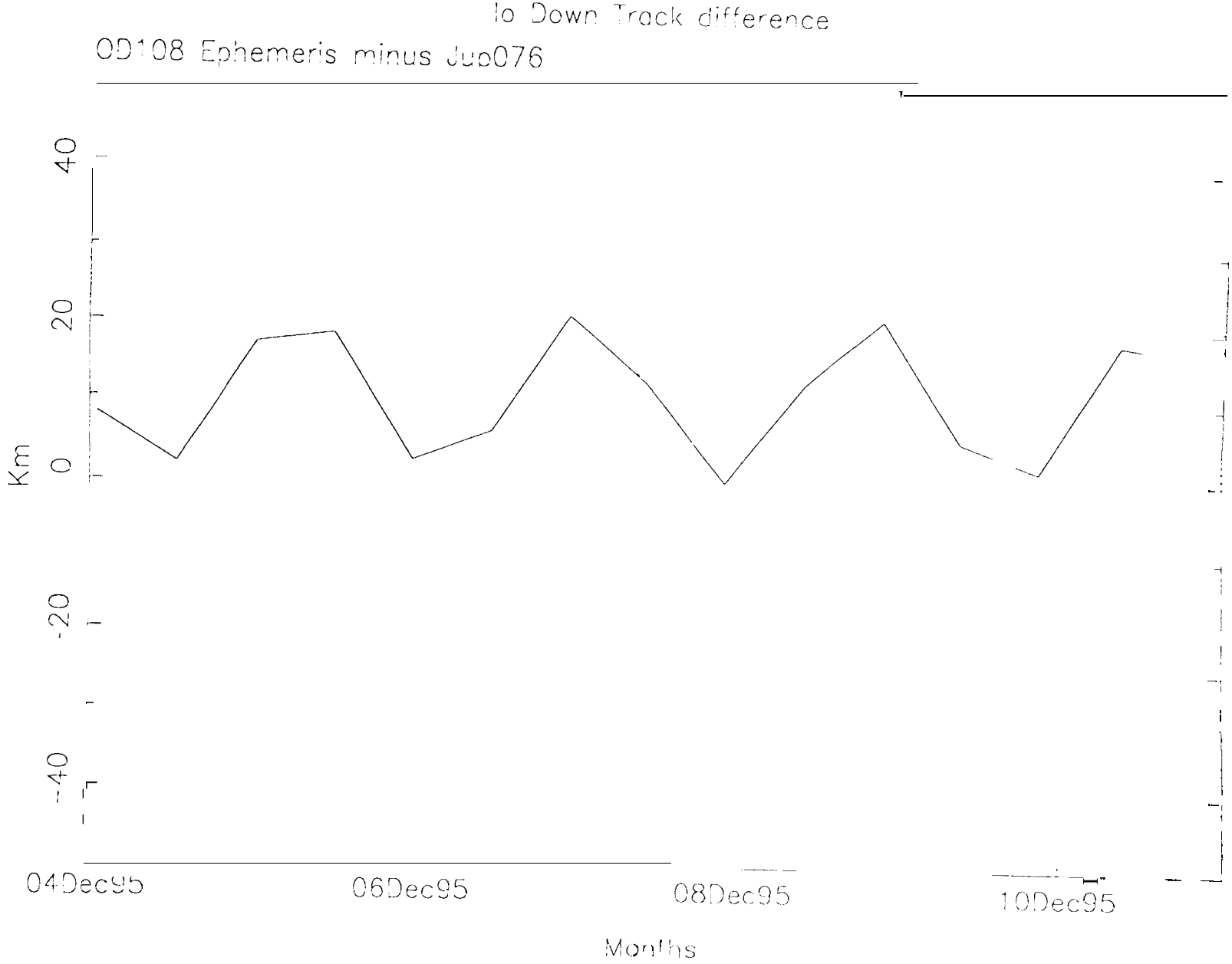
Io Down Track difference
OD108 Ephemeris minus Jup076
40
20
0
-20
-40
Km
04Dec95
06Dec95
08Dec95
10Dec95
Months

Fig ~~3b~~ 4b

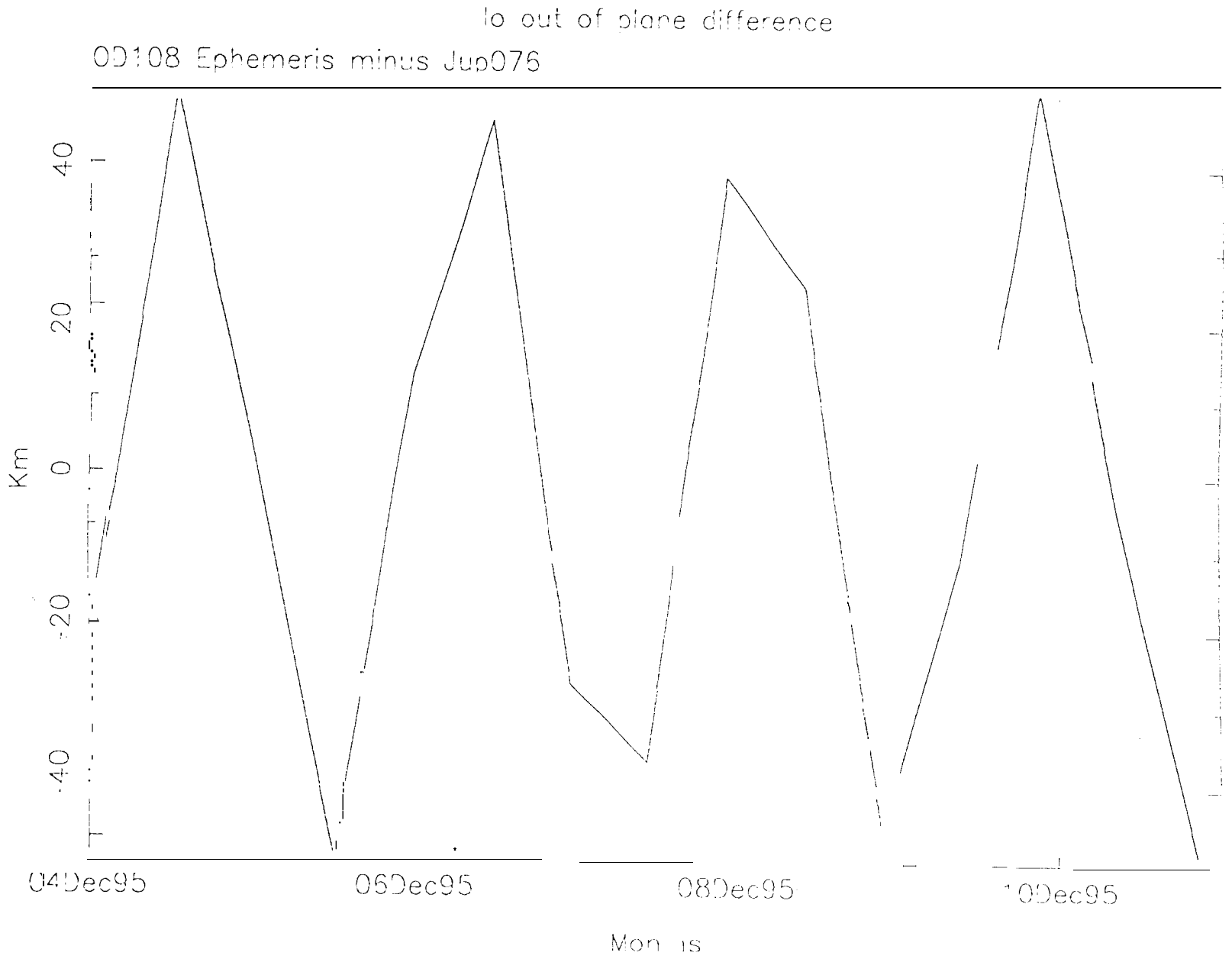
Io out of plane difference
OD108 Ephemeris minus Jup076
Km
40
20
0
-20
-40
04Dec95
06Dec95
08Dec95
10Dec95
Months

FIG ~~3c~~ 4c

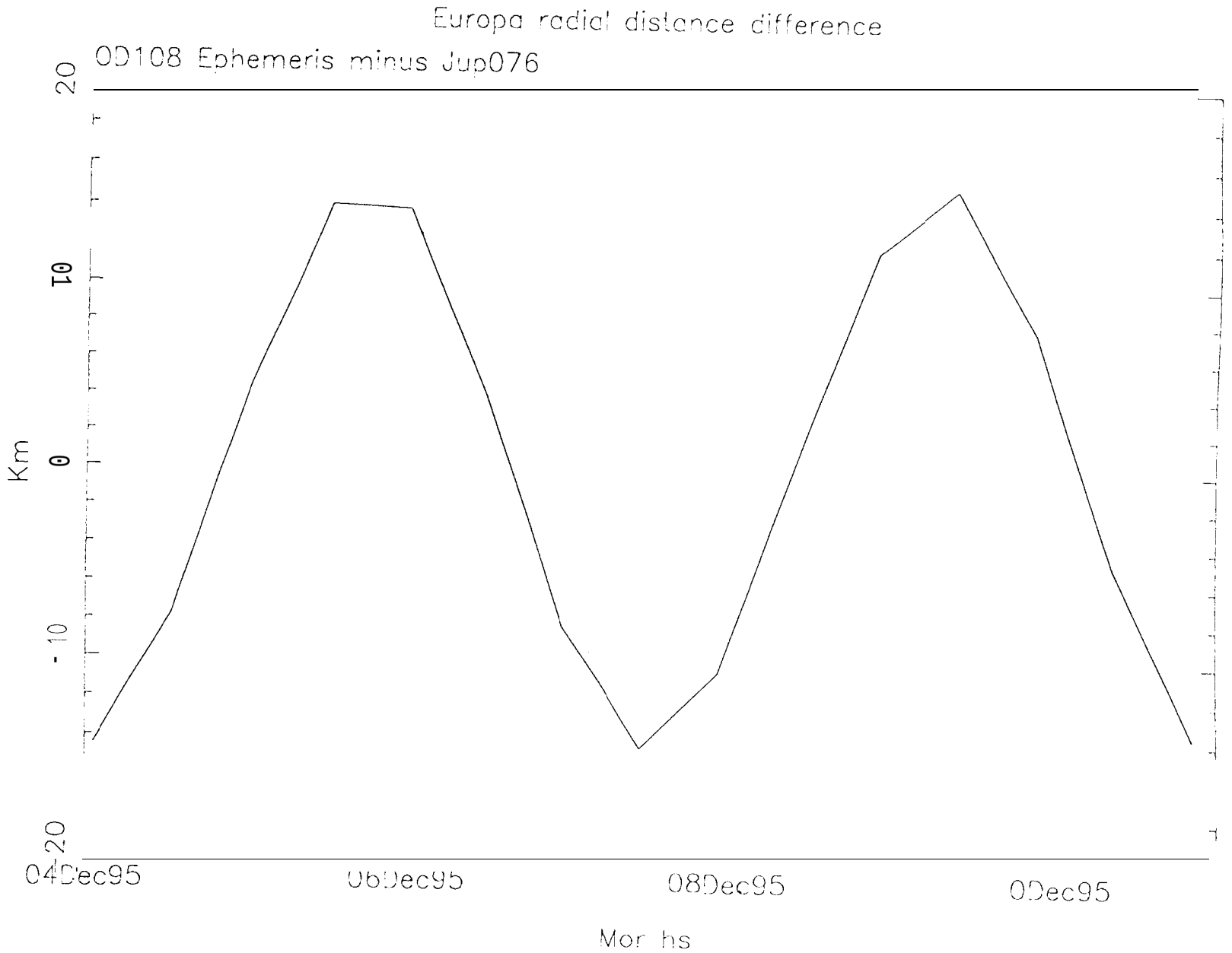
Europa radial distance difference
OD108 Ephemeris minus Jup076
20
10
0
- 10
20
Km
04Dec95
06Dec95
08Dec95
0Dec95
Mor hs

FIG ~~fjb4a~~ 5a

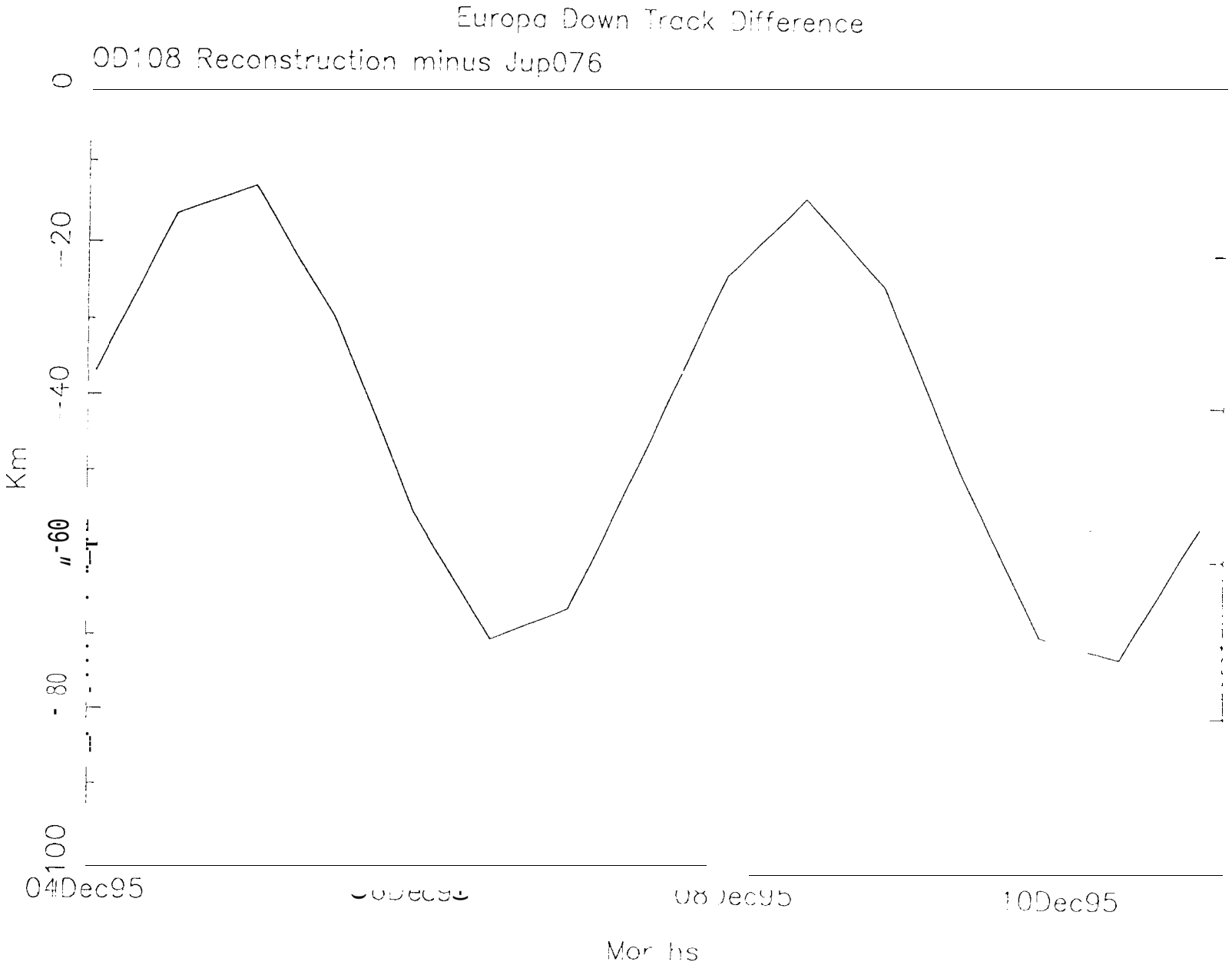
Europa Down Track Difference
OD108 Reconstruction minus Jup076
0
-20
-40
-60
-80
100
Km
04Dec95
08Dec95
10Dec95
Months

FIG ~~5A~~ 5b

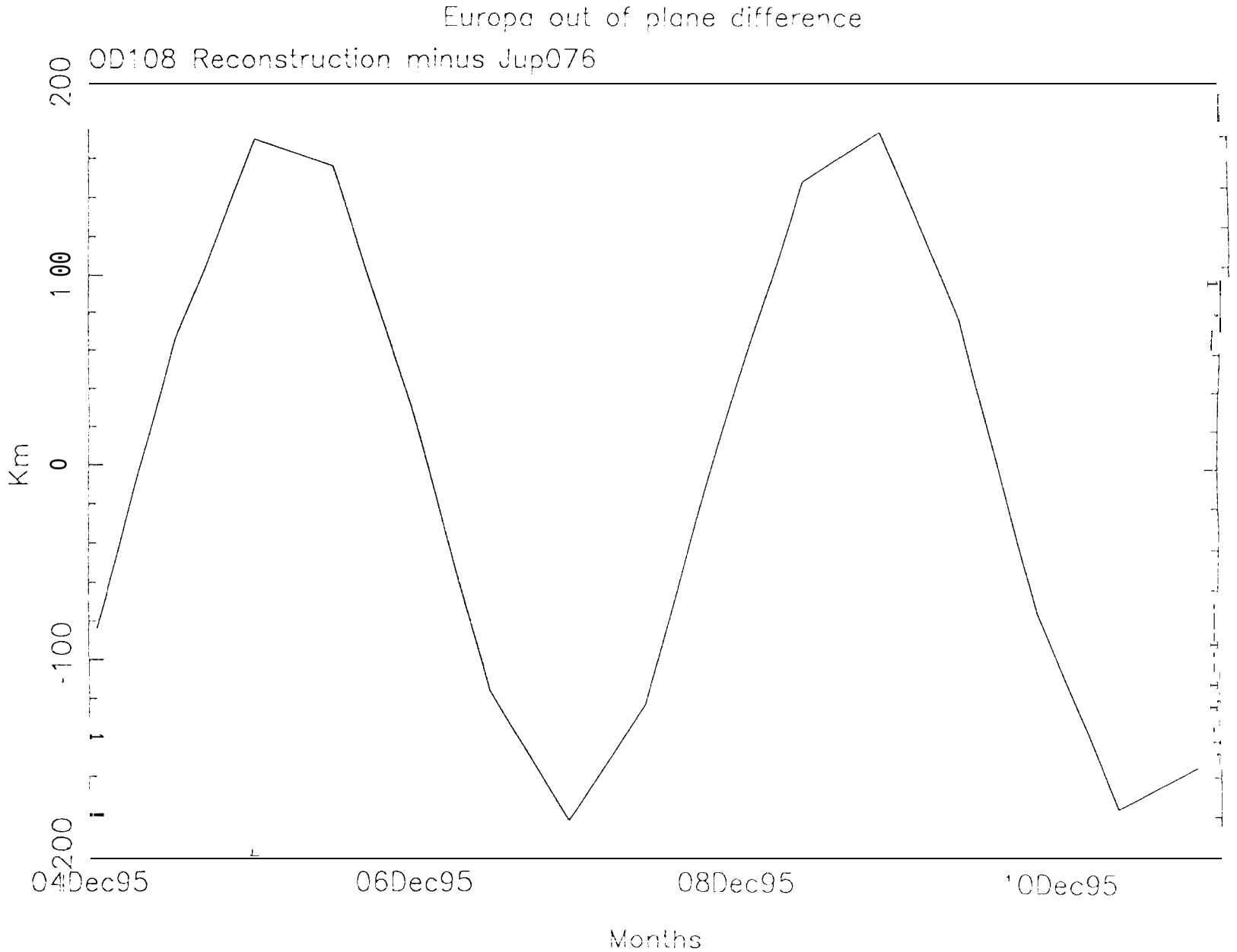
Europa out of plane difference
OD108 Reconstruction minus Jup076
200
100
0
-100
-200
Km
04Dec95
06Dec95
08Dec95
10Dec95
Months

FIG ~~4c~~ 5c

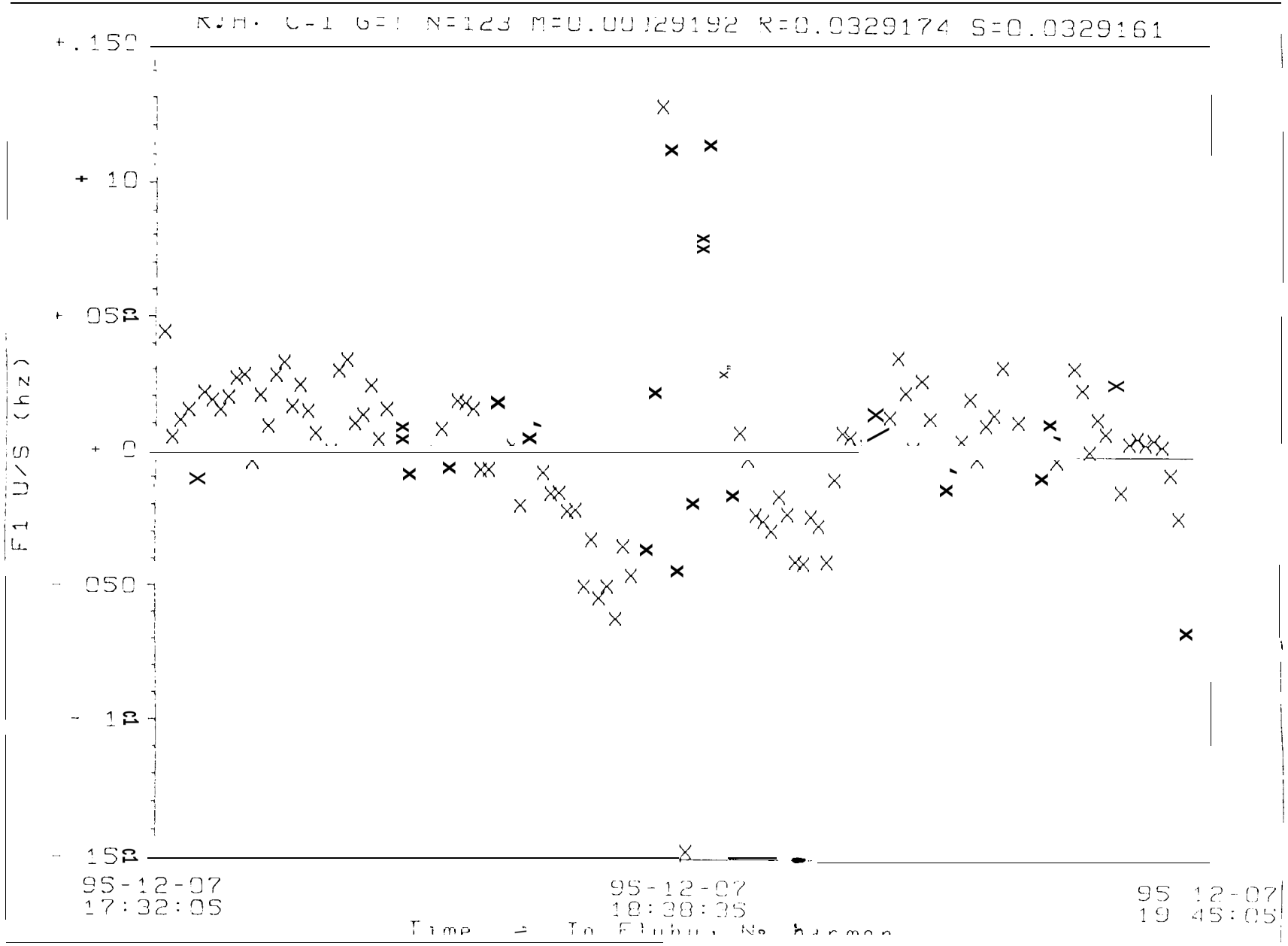
N=123 M=0.0029192 R=0.0329174 S=0.0329161
+.150
+ 10
+ 05
+ 0
- 05
- 10
- 15
F1 U/S (hz)
95-12-07
17:32:05
95-12-07
18:38:35
95-12-07
19:45:05
Time

FIG ~~5~~ 6

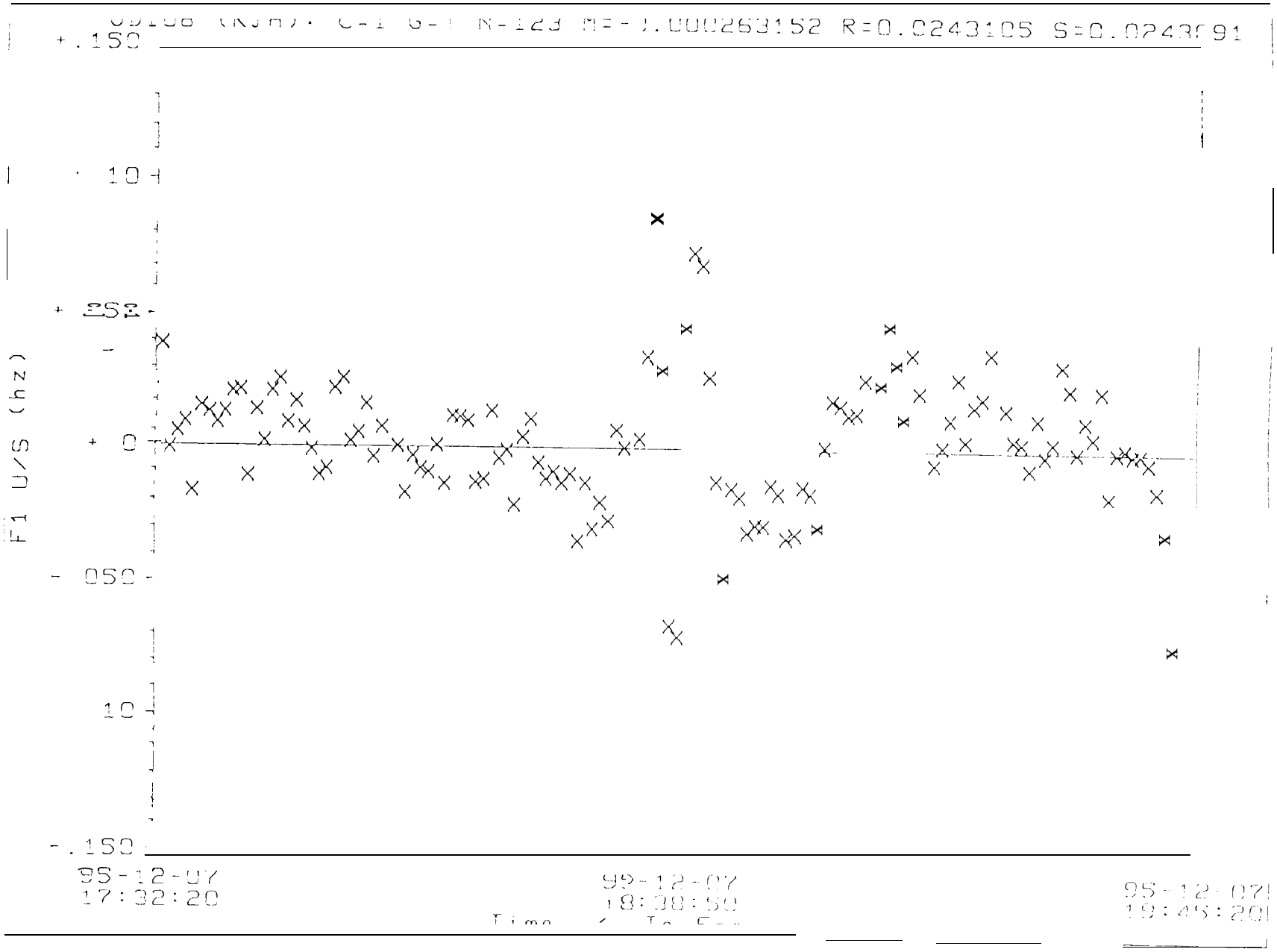
+.150
10
ESE
0
050
10
-.150
F1 U/S (hz)
95-12-07
17:32:20
95-12-07
18:38:50
95-12-07
19:45:20

FIG. ~~fib~~ 7

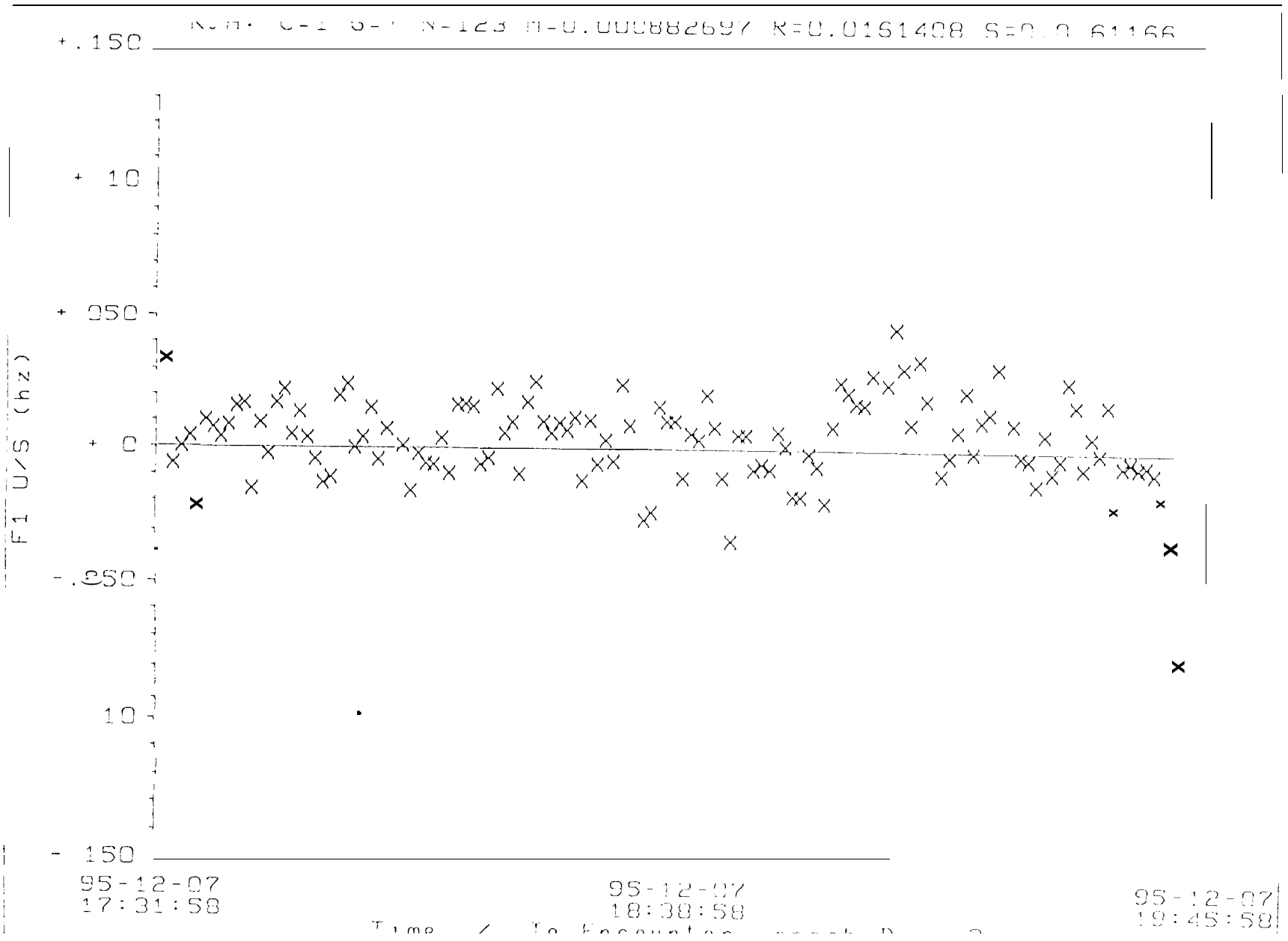
+.150
+ 10
+ 050
+ 0
-.050
- 10
- 150
F1 U/S (hz)
95-12-07
17:31:58
95-12-07
18:38:58
95-12-07
19:45:58

FIG. ~~7~~ 8

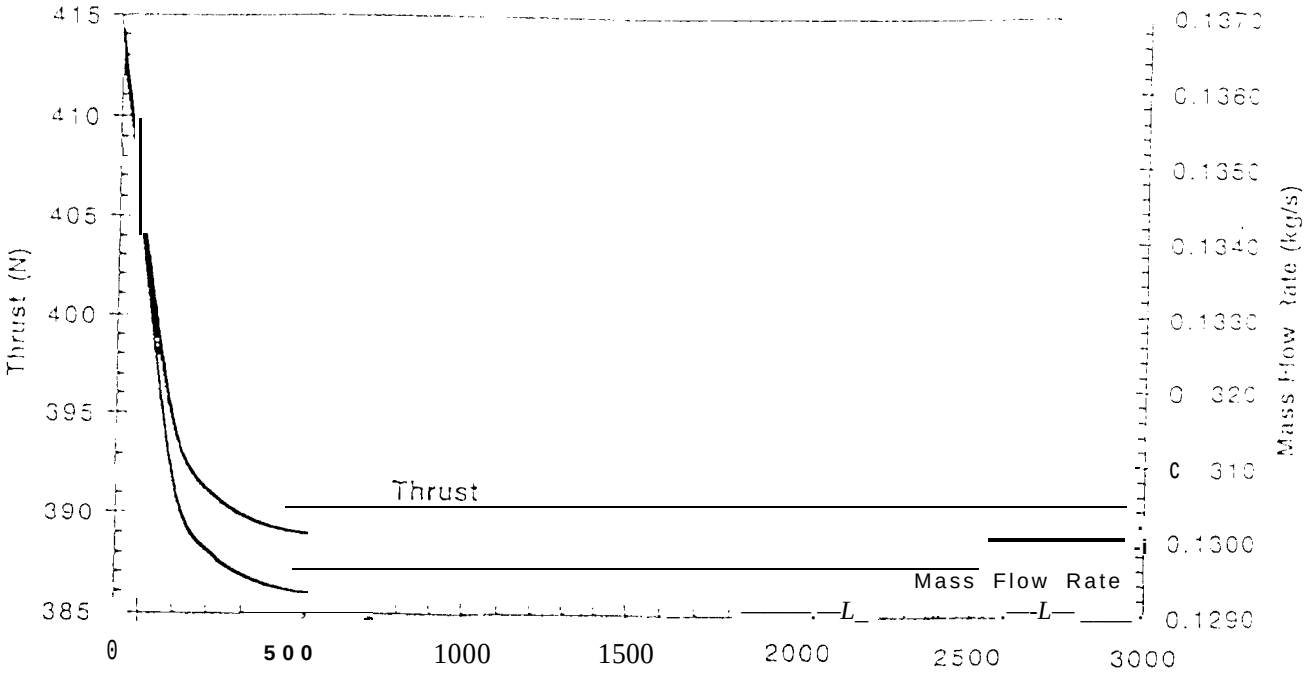
415
410
405
400
395
390
385
Thrust (N)
0.1370
0.1360
0.1350
0.1340
0.1330
0.1320
0.1310
0.1300
0.1290
Mass Flow Rate (kg/s)
Thrust
Mass Flow Rate
0
500
1000
1500
2000
2500
3000
Seconds Past Start of Burn

FIG. 9